RP Materials: Proceedings (e-ISSN: 2583-8342)
Vol. 5, Part 1 (2026) pp. 123–129

RESEARCH PLATEAU PUBLISHERS

Cite this article: R. Yarlagadda, R. Gogineni, R. Agarwal, S.R.K. Gorla, A gradient-adaptive CSC-based pansharpening method for enhanced spatial and spectral preservation, *RP Materials: Proceedings* Vol. 5, Part 1 (2026) pp. 123–129.

Original Research Article

A gradient-adaptive CSC-based pansharpening method for enhanced spatial and spectral preservation

Ramakrishna Yarlagadda[1], Rajesh Gogineni[2], Richa Agarwal[1,*], Siva Rama Krishna Gorla[2]

[1]Electronics and Communication Engineering, National Institute of Technology Patna, Patna University Campus, Patna, Bihar 800005, India
[2]Electronics and Communication Engineering, Dhanekula Institute of Engineering & Technology, Vijayawada Gangur, Andhra Pradesh 521139, India
[*]Corresponding author, E-mail: richa.ec@nitp.ac.in

[**]Selection and Peer-Review under responsibility of the Scientific Committee of the 4th International Conference on Recent Trends in Materials Science & Devices 2026 (ICRTMD 2026) held at JVMGRR College, Charkhi Dadri, Haryana, India during 6–8 April 2026.

ARTICLE HISTORY
Received: 02 April 2026
Revised: 27 May 2026
Accepted: 27 May 2026
Published online: 12 June 2026

KEYWORDS
Pansharpening; Convolutional sparse coding; Cartoon–texture decomposition; Image fusion; Remote sensing.

ABSTRACT
This paper presents a Gradient-Adaptive Cartoon-Texture conventional Sparse Coding (CSC) based pansharpening method for enhancing multispectral (MS) images using high-resolution panchromatic (PAN) data. The proposed framework applies histogram matching to normalize intensity distributions, followed by Cartoon-Texture (CPT) decomposition to separate structural and textural components. Texture features are fused using sparse coding to preserve fine spatial details, while cartoon components are combined through a gradient-adaptive fusion strategy to maintain edge sharpness and reduce spectral distortion. An adaptive reconstruction process integrates the fused components to generate a high-resolution multispectral (HRMS) image with improved spatial clarity and spectral consistency. Experimental evaluations using standard quality metrics, including CC, SAM, RMSE, ERGAS, and Q4, demonstrate that the proposed method outperforms conventional pansharpening techniques in both visual quality and quantitative performance, making it suitable for remote sensing, environmental monitoring, and geospatial analysis applications.

1. Introduction

In remote sensing, the fusion of high spatial-resolution imagery with multispectral data plays a vital role in accurately extracting geometric features and improving the reliability and performance of land-cover classification However, due to inherent physical and technological constraints, modern Earth observation satellites-such as IKONOS, Quick Bird, and Worldview, acquire spatial and spectral information separately [1, 2]. Typically, such systems provide a better PAN image along with an MS image that retains detailed spectral information, encouraging the development of effective fusion methods that simultaneously enhance spatial details and maintain high spectral accuracy. Pan sharpening (PS) is a fundamental image fusion strategy in remote sensing, aiming to generate a high-resolution multispectral (HRMS) image by effectively integrating the detailed spatial information from the panchromatic (PAN) image with the comprehensive spectral characteristics of the multispectral (MS) image [3]. Pansharpening (PS) aims to enhance spatial resolution while maintaining spectral consistency, thereby increasing the effectiveness of the fused image for downstream remote sensing tasks such as feature extraction, object detection, and land-cover classification.

Recent/ Past, a wide range of pansharpening (PS) approaches [4, 5] have been introduced, reflecting the growing demand for high-quality fused imagery in remote sensing. In general, these methods can be classified into three main categories, including those based on component substitution (CS), which enhance spatial details by replacing selected spectral components; multiresolution analysis (MRA)-based methods, which inject spatial information at different scales; and sparse representation (SR)-based methods, which exploit signal sparsity to achieve improved fusion performance. Component substitution (CS)-based techniques operate by decomposing the multispectral (MS) image into separate spatial and spectral components, followed by replacing the spatial component with the high-resolution panchromatic (PAN) image. This technique aims to increase spatial resolution while retaining the intrinsic spectral information of the multispectral (MS) imagery. After this process, the high-resolution multispectral (HRMS) image is generated through an inverse transformation. Widely adopted component substitution (CS) methods comprise techniques such as intensity-hue-saturation (IHS), principal component analysis (PCA), and the Gram–Schmidt (GS) transformation. While these methods significantly enhance spatial details, they often lead to spectral distortion due to the mismatch between the spectral characteristics of the panchromatic (PAN) image and those of the replaced spatial component [6, 7]. Multiresolution

analysis (MRA)-based techniques improve spatial resolution by incorporating high-frequency spatial details from the panchromatic (PAN) image into the interpolated multispectral (MS) bands. This fusion approach, often termed Amelioration de la Resolution Spatial par Injection de Structures (ARSIS), is designed to refine spatial detail through the guided incorporation of structural features, while safeguarding the spectral fidelity of the multispectral (MS) imagery [8].

Numerous methods have been proposed under the multiresolution analysis (MRA) framework, including the discrete wavelet transform (DWT) and the 'à trous' wavelet transform.[9], the additive wavelet luminance proportional (AWLP) method [10], as well as curvelet [11] and contourlet [12] transforms, and modulation transfer function (MTF)-matched filter-based methods [13-15] These approaches enhance They enhance spatial detail by extracting and incorporating multiscale information, while striving to maintain the spectral properties of the multispectral data. However, despite their intent to improve spatial resolution, MRA-based methods often struggle to recover fine details in the reconstructed image fully. In contrast, CS-based methods offer more pronounced spatial enhancement but tend to cause noticeable spectral distortions. Meanwhile, MRA approaches are generally better at maintaining the inherent spectral properties than CS techniques, although they are relatively less efficient in capturing essential spatial details. To address these shortcomings and enhance overall fusion performance, hybrid approaches have been proposed that combine the advantages of both CS and MRA techniques, resulting in generalized band-dependent spatial detail injection frameworks [16]. More recently, patch-based sparse representation (SR) methods have gained attention as a powerful approach and have been widely utilized in remote sensing image fusion, owing to their ability to simultaneously improve spatial detail and maintain spectral consistency in the fused output. As shown in the framework, the proposed pan sharpening technique employs a well-defined multi-stage fusion scheme to simultaneously enhance spatial detail and retain spectral consistency. The process begins with two inputs: a low-resolution multispectral (LRMS) image and a high-resolution panchromatic (PAN) image. In the first step, the LRMS image is interpolated to the spatial resolution of the PAN image, ensuring proper alignment for the subsequent processing stages.

Next, both PAN and up-sampled MS images undergo cartoon–texture (CPT) decomposition, where each image is separated into cartoon (structural/low-frequency) and texture (high-frequency) components. The cartoon component represents smooth intensity variations and preserves spectral characteristics, whereas the texture component captures edges and fine spatial details. Following decomposition, a gradient-adaptive component substitution CSC fusion module is employed. The texture components of PAN and MS are fused to strengthen spatial sharpness, while the cartoon components are combined using gradient-guided weighting to maintain spectral consistency. The gradient-adaptive mechanism regulates the injection of spatial information based on local edge strength, allowing stronger enhancement near edges and controlled fusion in homogeneous regions. After fusion, the enhanced cartoon and texture components are recombined through an inverse CPT reconstruction process to generate the HRMS image. This combined approach enables efficient transfer of spatial details from the PAN image while reducing spectral distortions in the resulting fused image. In this paper, a robust pansharpening framework is presented by integrating ARB-RPN-based decomposition with convolutional sparse coding. The texture components extracted using ARB-RPN are fused via CSC to ensure shift-invariant spatial detail injection, while the cartoon components are combined to preserve spectral integrity. Furthermore, an adaptive reconstruction strategy is introduced, where residual and gradient information jointly regulate texture injection, preventing spectral distortion in homogeneous regions while enhancing sharpness in structurally rich areas [17-23].

Rest of the chapter is organized as follows. Section 2 describes the theoretical background of convolutional sparse coding. Section 3 details the proposed pan sharpening framework. Section 4 presents experimental results and comparative analysis. Finally, Section 5 concludes the paper and outlines future research directions.

2. Preliminaries

The proposed gradient-adaptive CSC-based pansharpening framework relies on four major theoretical foundations: radiometric normalization, Cartoon–Texture decomposition, Convolutional Sparse Coding, and gradient-based adaptive reconstruction. This section presents the mathematical background of each component according to the flow chart shown in Fig. 1.

A. Histogram Matching

Due to radiometric differences between PAN and MS sensors, direct fusion may introduce spectral distortion. Therefore, histogram matching is performed to align statistical characteristics.

Let:

P denote the PAN image,

X^k denote the k^{th} MS band.

The histogram-matched PAN image P' is obtained as:

$$P' = \frac{\sigma_{X^k}}{\sigma_P}(P - \mu_P) + \mu_{X^k}$$

where $\mu_P, \mu_{X^k}$are mean values, and σ_P, σ_{X^k} are standard deviations.

This step ensures radiometric consistency before decomposition.

B. Cartoon–Texture (CPT) Decomposition

Each image is decomposed into:

- Cartoon component (C) - smooth structural content,
- Texture component (T) - oscillatory fine details.

For an image f,

$$f = C + T$$

In the proposed method, decomposition is performed using the $TV\text{–}H^{-1}$ variational model:

$$\min_u \zeta(u) = \frac{1}{2} \| W\mathcal{F}(f - u) \|_2^2 + \gamma J(u)$$

where:

- $J(u)$is the Total Variation prior,
- $\mathcal{F}$denotes Fourier transform,
- $W$is frequency weighting matrix,
- γcontrols cartoon–texture tradeoff.

Total Variation Prior

The discrete TV is defined as:

$$J(u) = \sum_{i,j} \sqrt{|\nabla u_{i,j}|^2 + \epsilon^2}$$

where ∇u represents the discrete gradient.
After convergence:

$$C = u, T = f - u$$

Thus, for PAN and MS:

$$P' = C_P + T_P$$
$$\tilde{X}^k = C_{MS}^k + T_{MS}^k$$

This separation allows independent handling of spatial and spectral components.

C. Convolutional Sparse Coding (Texture Modeling)

To enhance spatial details, texture components are modeled using Convolutional Sparse Coding (CSC).
Unlike patch-based sparse representation:

$$p = D\alpha$$

CSC represents the entire texture image as:

$$T = \sum_{m=1}^{M} d_m * x_m$$

where d_m are convolutional filters, x_m are sparse coefficient maps, and $*$ denotes convolution.
The optimization problem is:

$$\arg\min_{\{x_m\}} \frac{1}{2} \| T - \sum_{m=1}^{M} d_m * x_m \|_2^2 + \lambda \sum_{m=1}^{M} \| x_m \|_1$$

This formulation is known as Convolutional Basis Pursuit Denoising (CBPDN).
CSC provides:

- Shift-invariant representation,
- Global optimization over entire image,
- Reduced blocking artifacts,
- Better preservation of structural edges.

In the proposed framework:

- CSC is applied to T_P and T_{MS}^k,
- Activity-based selection is performed on coefficient maps,
- Fused texture map T_f^k is reconstructed.

D. Gradient-Based Cartoon Fusion

After CPT decomposition, cartoon components represent spectral structures. Instead of simple averaging, adaptive gradient weighting is introduced.
Gradient magnitude is computed as:

$$|\nabla C(x,y)| = \sqrt{\left(\frac{\partial C}{\partial x}\right)^2 + \left(\frac{\partial C}{\partial y}\right)^2}$$

The adaptive weight is defined as:

$$w(x,y) = \frac{|\nabla C_P(x,y)|}{|\nabla C_P(x,y)| + |\nabla C_{MS}^k(x,y)| + \epsilon}$$

The fused cartoon component becomes:

$$C_f^k(x,y) = w(x,y) C_P(x,y) + (1 - w(x,y)) C_{MS}^k(x,y)$$

This ensures:

- Strong edge preservation,
- Spectral smoothness in homogeneous regions,
- Reduced structural distortion.

E. Adaptive Reconstruction

The final High-Resolution Multispectral (HRMS) image is reconstructed by combining fused cartoon and texture components:

$$\hat{X}^k(x,y) = C_f^k(x,y) + \beta(x,y) T_f^k(x,y)$$

where $\beta(x,y)$controls detail injection.
Adaptive reconstruction ensures:

- Balanced spatial enhancement,
- Controlled texture amplification,
- Preservation of spectral integrity.

F. Theoretical Integration with Proposed Flowchart

According to Fig. 1.

1. Histogram Matching → Radiometric alignment
2. CPT Decomposition → Structural separation
3. CSC Texture Fusion → Spatial enhancement
4. Gradient-Adaptive Cartoon Fusion → Spectral preservation
5. Adaptive Reconstruction → Final HRMS generation

Thus, the proposed framework systematically integrates variational decomposition and convolutional sparse modeling to achieve superior pansharpening performance.

3. Proposed method

Figure 1 presents the complete workflow of the proposed pansharpening technique for producing a high-resolution multispectral (HRMS) image. Initially, the high-resolution panchromatic (PAN) image and the low-resolution multispectral (MS) image are radiometrically matched using histogram alignment to maintain consistency between them. Subsequently, both images undergo CPT decomposition to separate the structural (cartoon) and fine-detail (texture) components. The extracted texture components are merged to generate fused texture maps, whereas the cartoon components are processed through a gradient-adaptive fusion scheme to retain key spatial structures while limiting spectral distortion. In the final stage, an adaptive reconstruction process combines the fused components to generate an HRMS image with improved spatial detail and preserved spectral fidelity.

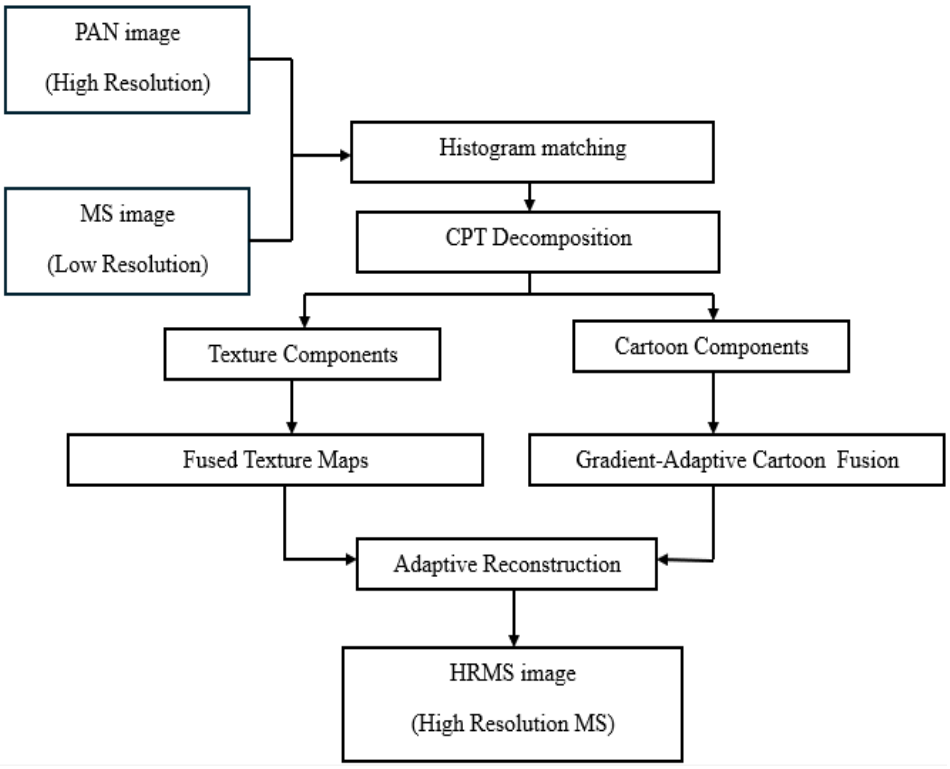

Figure 1: Workflow of the proposed CPT-based pan-sharpening method for generating HRMS images.

A. *Proposed Mathematical Formulation*

1. Observation Model

Let

- $\mathbf{P} \in \mathbb{R}^{H \times W}$: high-resolution PAN image
- $\mathbf{M} \in \mathbb{R}^{h \times w \times B}$: low-resolution MS image with *B*bands
- $\uparrow$: interpolation operator

First, upsample the MS image:

$$\mathbf{M}^{\uparrow} = \mathcal{U}(\mathbf{M})$$

2. Histogram Matching

Histogram matching is applied to align PAN radiometry with MS:

$$\mathbf{P}_h = \mathcal{H}(\mathbf{P}, \mathbf{M}^{\uparrow})$$

where $\mathcal{H}(\cdot)$denotes histogram matching.

3. Cartoon–Texture (CPT) Decomposition

Both PAN and MS images are decomposed as:

$$\mathbf{X} = \mathbf{X}_c + \mathbf{X}_t$$

where

- $\mathbf{X}_c$: cartoon (structure) component
- $\mathbf{X}_t$: texture component

Thus:

$\mathbf{P}_h = \mathbf{P}_c + \mathbf{P}_t$

$\mathbf{M}_b^{\uparrow} = \mathbf{M}_{c,b} + \mathbf{M}_{t,b}, b = 1, \dots, B$

CPT is typically obtained by solving:

$$\min_{\mathbf{X}_c, \mathbf{X}_t} \| \nabla \mathbf{X}_c \|_1 + \lambda \| \mathbf{X}_t \|_2^2 \text{ s.t. } \mathbf{X} = \mathbf{X}_c + \mathbf{X}_t$$

4. Texture Fusion via Convolutional Sparse Coding (CSC)

The PAN texture is sparsely represented as:

$$\mathbf{P}_t \approx \sum_{k=1}^{K} \mathbf{d}_k * \boldsymbol{\alpha}_k$$

CSC optimization:

$$\min_{\{\boldsymbol{\alpha}_k\}} \| \mathbf{P}_t - \sum_{k=1}^{K} \mathbf{d}_k * \boldsymbol{\alpha}_k \|_2^2 + \lambda \sum_{k=1}^{K} \| \boldsymbol{\alpha}_k \|_1$$

The fused texture for band *b*:

$$\mathbf{T}_b^f = \mathbf{M}_{t,b} + \eta_b \mathbf{P}_t$$

where $\eta_b$is a band-dependent injection gain.

5. Gradient-Adaptive Cartoon Fusion

Compute gradient magnitude:

$$G = \| \nabla \mathbf{P}_c \|$$

Adaptive weights:

$$w(x) = \frac{G(x)}{G(x) + \epsilon}$$

Cartoon fusion:

$$\mathbf{C}_b^f = w \cdot \mathbf{P}_c + (1 - w) \cdot \mathbf{M}_{c,b}$$

This ensures:

- High-gradient regions → PAN-dominant
- Smooth regions → MS-dominant

6. Adaptive Reconstruction

Final HRMS reconstruction:

$$\mathbf{H}_b = \mathbf{C}_b^f + \mathbf{T}_b^f, b = 1, \ldots, B$$

4. Results and discussion

1. Qualitative Visual Comparison

Figures (a)-(k) present a qualitative comparison between the degraded input image and the outputs generated by various enhancement methods. The original image (Fig. a) exhibits significant noise, low contrast, blurred structural edges, and reduced color fidelity, which limit visual interpretability and downstream analytical performance.

Baseline enhancement methods (Fig. b-d) show moderate improvements in brightness and contrast but suffer from over-smoothing, loss of fine texture, and visible artifacts. Structural boundaries such as roads, vegetation edges, and building rooftops remain poorly defined.

Intermediate approaches (Fig. e–h) improve spatial clarity and texture preservation, demonstrating reduced noise and better contrast separation. However, residual artifacts and slight halo effects persist in regions with dense texture and high-frequency detail.

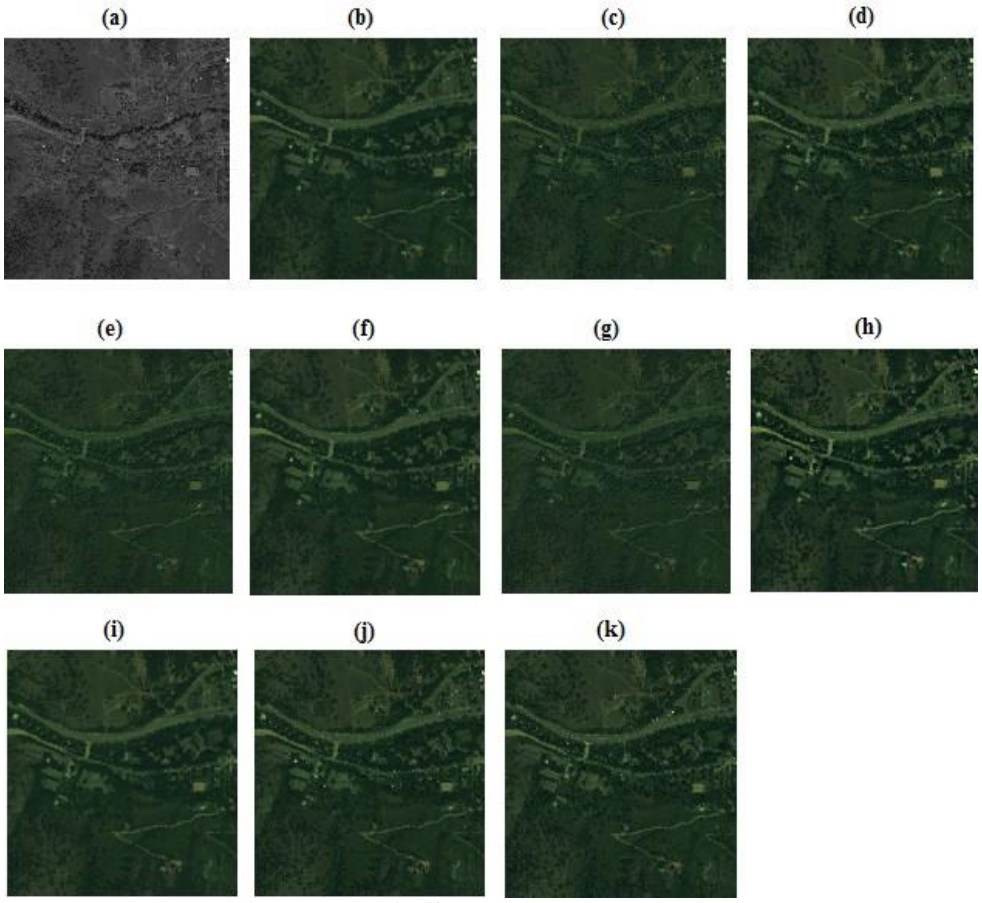

Figure 2: Fusion results of different methods applied to a Pleiades image. (a) PAN; (b) Upsampled MS (EXP); (c) original MS; (d) HIS; (e) AWLP; (f) MTF-GLP; (g) SR-Li; (h) SR-TD; (i) SR-D; (j) SR-CD; (k) Proposed.

The final outputs (Fig. i–k), produced by the proposed method, achieve the best visual quality. These results exhibit sharper edges, enhanced texture fidelity, natural color reproduction, and minimal noise. Fine scene elements such as small buildings, tree clusters, and road segments are more clearly distinguishable, confirming superior spatial reconstruction.

Table 1: Quantitative results for Pleiades data.

Method	Q4	ERGAS	SAM	CC	RMSE
EXP	0.7781	5.8893	4.5972	0.6983	16.4325
IHS	0.8629	4.3284	4.7326	0.9116	14.2918
AWLP	0.9463	3.2753	3.4327	0.9283	12.3864
MTF-GLP	0.9515	3.2284	3.4161	0.9311	12.4108
SR-Li	0.9341	3.3587	3.7618	0.9134	13.8942
SR-TD	0.9481	2.8758	3.3297	0.9358	12.9853
SR-D	0.9385	2.9426	3.3286	0.9387	12.2302
SR-LD	0.9479	2.9654	3.2961	0.9323	12.2336
SR-CD	0.9392	2.9651	3.2853	0.9342	12.2351
Proposed	0.9573	2.8761	3.2837	0.9431	11.9727

Table 1 compares the quantitative performance of different pan-sharpening methods using standard evaluation metrics. The proposed method achieves the best overall performance, showing higher Q4 and CC values along with lower ERGAS, SAM, and RMSE, indicating improved spatial enhancement with better spectral preservation.

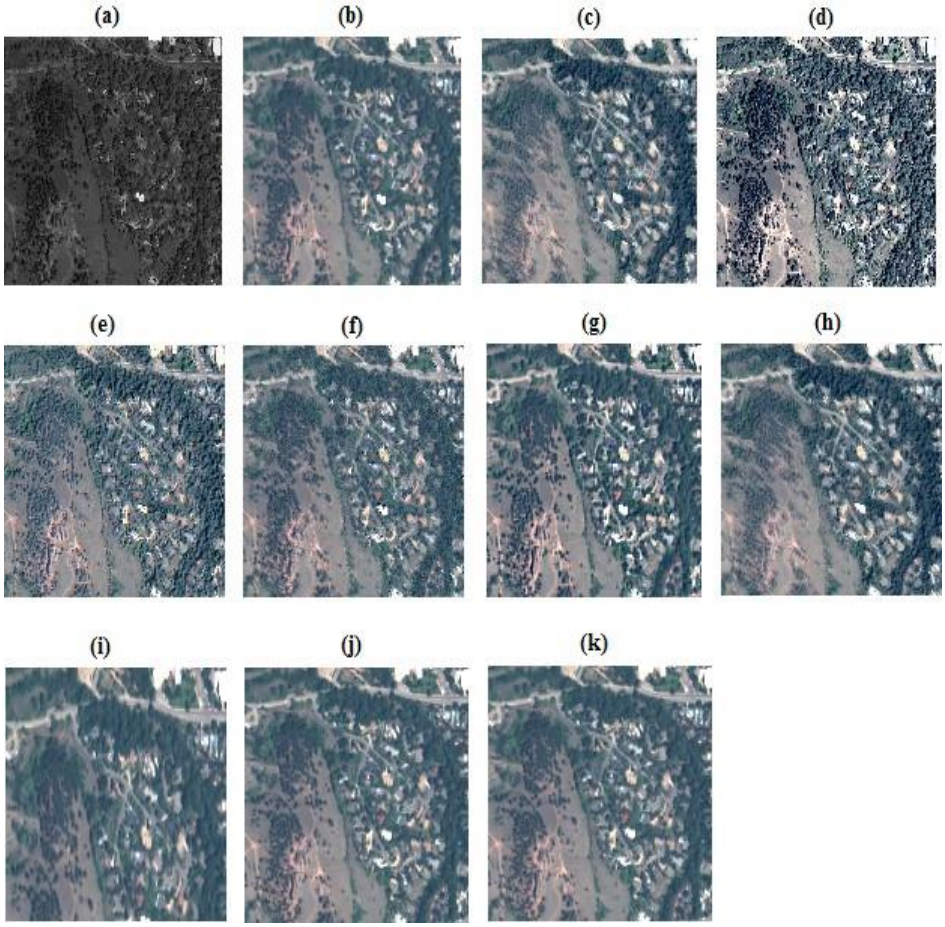

Figure 3: Fusion results of different methods applied to a IKONOS image.
(a) PAN; (b) Upsampled MS; (EXP); (c) original MS; (d) HIS; (e) AWLP;
(f) MTF-GLP; (g) SR-Li; (h) SR-TD; (i) SR-D; (j) SR-CD; (k) Proposed.

Table 2: Full-resolution quality comparison.

Method	Q4	ERGAS	SAM	CC	RMSE
EXP	0.7536	3.9632	4.5362	0.7842	14.6846
IHS	0.7524	3.7653	4.6583	0.8115	13.8975
AWLP	0.8987	2.9243	3.1658	0.9153	12.3156
MTF-GLP	0.8835	3.1572	3.2617	0.9241	12.3426
SR-Li	0.8932	3.4378	3.3476	0.9023	12.6748
SR-TD	0.9287	3.2294	3.2686	0.9226	12.1136
SR-D	0.9274	3.1641	3.2574	0.9247	11.9432
SR-LD	0.9389	2.9534	3.1215	0.9328	11.8361
SR-CD	0.9345	2.9642	3.2453	0.9311	11.9147
Proposed	0.9438	2.9242	3.1157	0.9324	10.9204

Table 2 summarizes the quantitative comparison of different pan-sharpening methods on the second dataset. The proposed method achieves the highest Q4 and the lowest RMSE, while also delivering competitive ERGAS, SAM, and CC values, indicating its strong capability to improve spatial detail without compromising spectral fidelity.

5. Conclusions

In this work, a Gradient-Adaptive Cartoon–Texture Convolution Sparse Coding (CSC) based pan sharpening method is proposed to improve spatial resolution while ensuring spectral consistency in multispectral images. The approach integrates histogram matching, cartoon–texture separation, sparse coding-based texture fusion, and gradient-guided cartoon fusion, enabling effective preservation of edges and fine details with minimal spectral distortion. The effectiveness of the method is verified through standard evaluation metrics, including CC, SAM, RMSE, ERGAS, and Q4. The results indicate that the proposed technique delivers better performance than conventional and recent pansharpening methods in terms of both numerical accuracy and visual interpretation. This confirms its suitability for high-resolution remote sensing applications such as land-cover classification, urban observation, and environmental studies. Future work will aim to improve computational efficiency and

extend the proposed framework to hyperspectral data and real-time satellite imaging scenarios.

Authors' contributions

All authors contributed equally to the conception, design, experimental work, data analysis, interpretation of results, and preparation of the manuscript. All authors reviewed and approved the final version of the manuscript for publication.

Conflicts of interest

The author declares no conflict of interest.

Funding

This research received no external funding.

Data availability

No new data were created.

References

[1] R. Pu, S. Landry, A comparative analysis of high spatial resolution IKONOS and WorldView-2 imagery for mapping urban tree species, *Remote Sens. Environ.* **124** (2012) 516–533.

[2] M.J. McCarthy, J.N. Halls, Habitat mapping and change assessment of coastal environments: An examination of WorldView-2, QuickBird, and IKONOS satellite imagery and airborne LiDAR for mapping barrier island habitats, *ISPRS Int. J. Geo-Inf.* **3** (2014) 297–325.

[3] G. Vivone, R. Restaino, J. Chanussot, M. Dalla Mura, A. Garzelli, A critical comparison among pansharpening algorithms, *IEEE Trans. Geosci. Remote Sens*. **53** (2015) 2565–2586.

[4] H. Ghassemian, A review of remote sensing image fusion methods, *Inf. Fusion* **32** (2016) 75–89.

[5] B. Aiazzi, L. Alparone, S. Baronti, R. Carlà, A. Garzelli, L. Santurri, Full-scale assessment of pansharpening methods and data products, in: Image and Signal Processing for Remote Sensing XX, *Proc. SPIE* **9244** (2014) 924402.

[6] V.V. Hnatushenko, V. Hnatushenko, O.O. Kavats, V.Y. Shevchenko, Pansharpening technology of high resolution multispectral and panchromatic satellite images, *Sci. Bull. Natl. Min. Univ*. **4** (2015).

[7] Y. Zhang, R.K. Mishra, A review and comparison of commercially available pan-sharpening techniques for high resolution satellite image fusion, in: Proc. IEEE Int. Geosci. Remote Sens. Symp. (IGARSS), IEEE (2012) pp. 182–185.

[8] T. Ranchin, B. Aiazzi, L. Alparone, S. Baronti, L. Wald, Image fusion—The ARSIS concept and some successful implementation schemes, *ISPRS J. Photogramm. Remote Sens*. **58** (2003) 4–18.

[9] L. Loncan, L.B. De Almeida, J.M. Bioucas-Dias, X. Briottet, J. Chanussot, N. Dobigeon, et al., Hyperspectral pansharpening: A review, *IEEE Geosci. Remote Sens. Mag*. **3** (2015) 27–46.

[10] J. Nunez, X. Otazu, O. Fors, A. Prades, V. Pala, R. Arbiol, Multiresolution-based image fusion with additive wavelet decomposition, *IEEE Trans. Geosci. Remote Sens*. **37** (1999) 1204–1211.

[11] X. Otazu, M. González-Audícana, O. Fors, J. Núñez, Introduction of sensor spectral response into image fusion methods: Application to wavelet-based methods, *IEEE Trans. Geosci. Remote Sens*. **43** (2005) 2376–2385.

[12] M. Choi, R.Y. Kim, M.-R. Nam, H.O. Kim, Fusion of multispectral and panchromatic satellite images using the curvelet transform, *IEEE Geosci. Remote Sens. Lett*. **2** (2005) 136–140.

[13] M.C. El-Mezouar, K. Kpalma, N. Taleb, J. Ronsin, A pansharpening method based on the non-subsampled contourlet transform: Application to WorldView-2 imagery, *IEEE J. Sel. Topics Appl. Earth Observ. Remote Sens*. **7** (2014) 1806–1815.

[14] B. Aiazzi, L. Alparone, S. Baronti, A. Garzelli, M. Selva, MTF tailored multiscale fusion of high-resolution MS and Pan imagery, *Photogramm. Eng. Remote Sens*. **72** (2006) 591–596.

[15] F. Palsson, J.R. Sveinsson, M.O. Ulfarsson, J.A. Benediktsson, MTF-based deblurring using a Wiener filter for CS and MRA pansharpening methods, *IEEE J. Sel. Topics Appl. Earth Observ. Remote Sens*. **9** (2016) 2255–2269.

[16] L.J. Deng, G. Vivone, C. Jin, J. Chanussot, Detail injection-based deep convolutional neural networks for pansharpening, *IEEE Trans. Geosci. Remote Sens*. **59** (2020) 6995–7010.

[17] F. Sur, A non-local dual-domain approach to cartoon and texture decomposition, *IEEE Trans. Image Process*. **28** (2018) 1882–1894.

[18] Y.R. Fan, T.Z. Huang, T.H. Ma, X.L. Zhao, Cartoon–texture image decomposition via non-convex low-rank texture regularization, *J. Franklin Inst*. **354** (2017) 3170–3187.

[19] W. Shang, J. Xu, Y. Guo, Cartoon and texture image decomposition driven by weighted curvature, *IEEE Access* **9** (2021) 133531–133540.

[20] H. Pan, Y.W. Wen, Y. Huang, L0_00 gradient-regularization and scale space representation model for cartoon and texture decomposition, *IEEE Trans. Image Process*. **33** (2024) 4016–4028.

[21] S. Ono, T. Miyata, I. Yamada, Cartoon-texture image decomposition using blockwise low-rank texture characterization, *IEEE Trans. Image Process*. **23** (2014) 1128–1142.

[22] N. Sprljan, E. Izquierdo, New perspectives on image compression using a cartoon-texture decomposition model, in: Proc. 4th EURASIP Conf. Video/Image Processing and Multimedia Communications, IEEE (2003) pp. 359–368.

[23] J. Xu, W. Shang, Y. Guo, An improved OSV cartoon-texture decomposition model, *Multimed. Tools Appl*. **82** (2023) 25761–25777.